Sodankylä Geophysical Observatory Publications (2003) 92:109–112

All-Sky Imaging Within the Canadian CANOPUS and NORSTAR Projects

Eric F. Donovan, Trond S. Trondsen, Leroy L. Cogger, and Brian J. Jackel

Institute for Space Research, University of Calgary, Alberta, Canada

Received: 7.12.2001 – Accepted: 23.9.2002

1 Introduction

A digital All-Sky Imager (ASI) was operated at Gillam Manitoba, as part of the CANOPUS program, from 1986 until April 2001. In the fall of 2000, three new ASIs were deployed (one each at Gillam, Rankin Inlet, and Resolute Bay) as the first phase of the Canadian NORSTAR project. In this paper we outline the technical specifications of the original CANOPUS imager, the first generation of NORSTAR ASIs, and our method of calibrating the NORSTAR imagers. We also describe the CANOPUS ASI data set, the scientific progress that it has facilitated, and the scientific objectives of the NORSTAR program. The NORSTAR image data set will provide important ground-based optical observations that can be used in conjunction with data from the ongoing CLUSTER II mission, as well as the upcoming Magnetospheric Multiscale mission.

2 The CANOPUS Gillam ASI

The CANOPUS array was deployed across North-Western Canada in the late 1980s as the Canadian contribution to the OPEN (Origin of Plasmas in the Earth's Neighbourhood) program (Rostoker et al., 1995). Until last year, CANOPUS consisted of thirteen magnetometers and riometers, four Meridian Scanning Photometers (MSPs), and one digital All-Sky Imager (see Figure 1). The ASI was operated from 1986 to 2001. It was located at Gillam so that its field of view (FOV) was within the intersecting beams of the VHF Bistatic Auroral Radar (BARS), which operated until 1993.

This ASI was designed and built at the University of Calgary. It consists of a 256×256 pixel intensified CCD, a fish-eye lens followed by telecentric optics and a four-position filterwheel with narrow-band 2-inch diameter interference filters. Originally, the ASI employed pixel binning to generate 16×25 pixel low-resolution images which were ideal as an overlay for BARS data. In 1992, it was put into a high-resolution mode, and has from that point on delivered full 256×256 images, yielding a spatial resolution at auroral altitudes of a few kilometers. The integration time is ∼1.6 seconds, and images are cropped radially at a zenith angle of ∼70 degrees. Normal image repetition rate in later years has been one 557.7 nm and one 630.0 nm image per minute. Once each hour dark frame data is acquired with the shutter closed, and a "starfield" image is taken through an open filterwheel position. These help with determination of absolute brightnesses and pixel positioning, respectively.

Correspondence to: E.F. Donovan

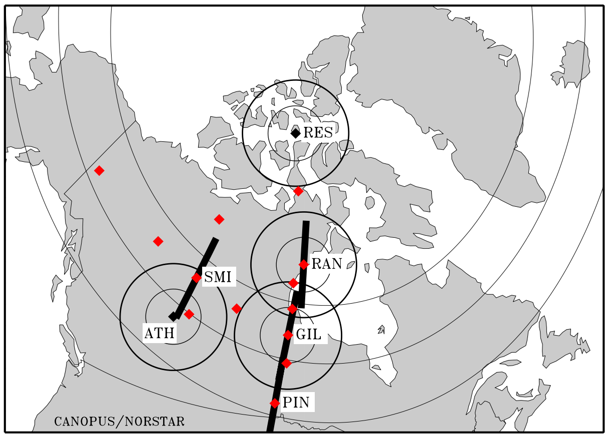

Fig. 1. FOVs of CANOPUS/NORSTAR ASIs and MSPs. Optical stations are labelled with the three letter abbreviations for the site names. Small and large circles indicate ASI FOVs assuming altitudes of 110 km and 230 km, respectively. The MSP FOVs, presuming an emission height of 110 km, are indicated by the thick black lines aligned roughly north-south. Red diamonds indicate the location of CANOPUS magnetometers. Contours of constant invariant latitude (60°, 65°, 70°) are also shown.

The ASI FOV covers invariant latitudes ranging from ∼64° to ∼70°, assuming emissions from 110 km. Images typically contain aurora on field lines threading the inner CPS, although in geomagnetically active periods the boundary between open and closed field lines is often within (or even equatorwad of) the FOV (see Figure 2 and the discussion in

Zesta et al. (2000)).

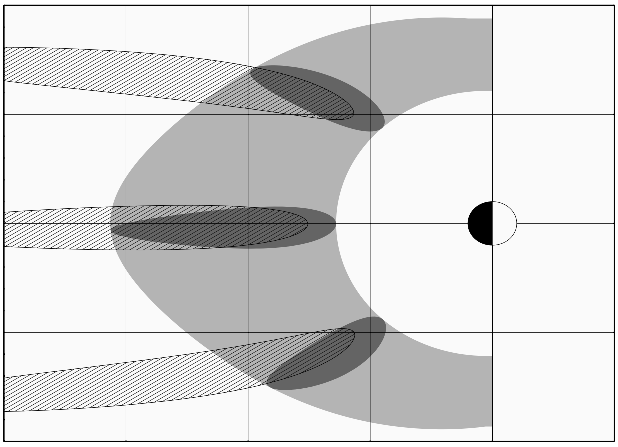

Fig. 2. ASI 110 km FOV mapped to the equatorial plane using the T87 model. Shaded and cross-hatched distorted ovals indicate the FOV at 21, 00 and 03 MLT for the Kp=0 and Kp=3 models, respectively. Also shown is the area swept out by the FOV (T87 Kp=0) between dusk and dawn.

Although optical coverage of the BARS FOV was the primary motivation for the ASI location, the unique observational contribution of the CANOPUS ASI project was ultimately due to its location on the Churchill meridian line of magnetometers and MSPs (see Figure 1). In particular, the MSP data allowed for the placing of the ASI images within a larger context of magnetospheric precipitation (Voronkov et al., 1999, e.g.).

The high resolution 557.7 nm data set has been widely used. It consists of eight years of roughly 60 000 images per year. Figure 3 is comprised of CANOPUS ASI images of a variety of interesting auroral forms. Scientific uses of this data have included: 1) demonstrating that large aspect angle VHF radio auroral echoes can often be a result of anomalously large refraction of the radio waves due to ionisation caused by discrete auroral precipitation (Hall et al., 1990; Prikryl and Cogger, 1991); 2) a survey of the widths of mesoscale auroral arcs that has been useful in constraining auroral arc theories (Knudsen et al., 2001); 3) studies of the evolution of auroral vortices during pseudobreakups and the substorm expansive phase (Samson et al., 1996; Voronkov et al., 2000); the first ever unambiguous identification of an optical signature of BBFs in the CPS (Zesta et al., 2000); development work on an *auroral tracker* (Syrjäsuo and Donovan, 2001). Ongoing research involving this data set is focussed on auroral streamers, pulsating aurora, the two dimensional structure of PBIs, and substorms.

3 The NORSTAR Array

In the fall of 2000, three new ASIs were deployed, one each at Gillam, Rankin Inlet, and Resolute Bay (Figure 1). In January of 2002, the original CANOPUS ASI will be redeployed at Athabasca (Figure 1). We have plans to build and deploy

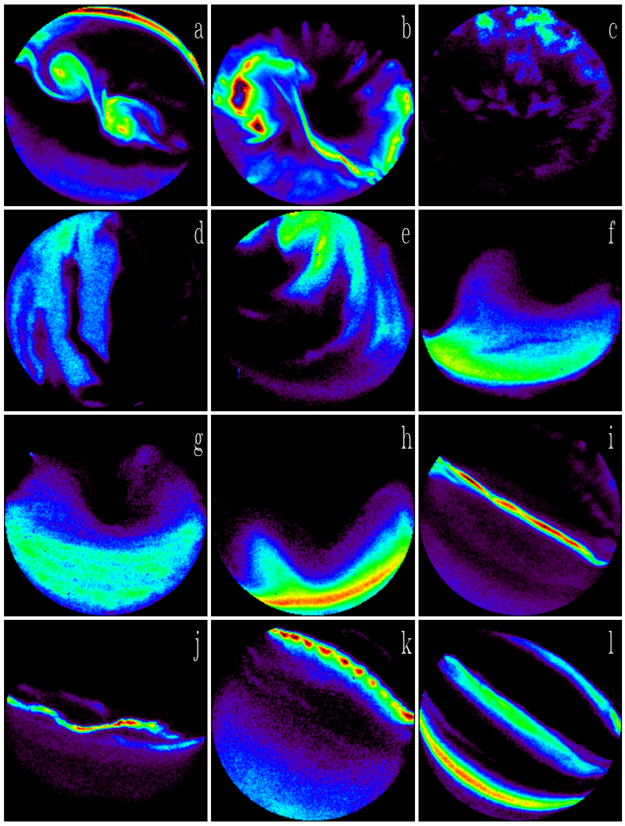

Fig. 3. Examples of 558 nm CANOPUS ASI images (North and East are up and right, respectively): a-b) spirals; c-d) pulsating aurora; e) streamers; f-h) Omega bands/torches; i-l) mesoscale arcs.

at least two more imagers over the next few years. This new array of imagers is called NORSTAR (for NORthern Solar Terrestrial ARray). The operational objective of NORSTAR is to provide quantitative mesoscale auroral image mosaics, at a number of scientifically relevant wavelengths, and at relatively high time resolution (ie., one frame every ∼20 seconds, for each wavelength). NORSTAR mosaics will provide quantitative, two dimensional maps of auroral emissions, from equatorward of the auroral oval, into the polar cap, and over several hours of MLT. The combined NORSTAR FOV will overlap with with the Canadian SuperDARN radar FOVs, and with the region covered by existing CANOPUS magnetometers, riometers, and MSPs. The large geographical area of the combined NORSTAR imager FOVs will allow for a large number of satellite conjunctions, as well for the following of the evolution of mesoscale structures that are often either larger than the FOV of a single imager, or move outside of the FOV (see the discussion of vortex evolution in Voronkov et al. (2000)). NORSTAR data will facilitate both stand-alone science and support Canadian involvement in coordinated observations involving the ESA Cluster II program, and possible new NASA MIDEX magnetospheric missions. Viewing conditions permitting, NORSTAR will operate continuously for at least three years, and hopefully longer.

The Rankin Inlet ASI is located directly under the intersection of the Saskatoon and Kapuskasing SuperDARN HF radar beams. As well, since Rankin Inlet is at ~74° invariant latitude, the boundary between open and closed field lines is often within the ASI FOV. Resolute Bay is nearly always located in the polar cap, and features such as 630 nm patches and polar cap arcs are often observed. The scientific advantages afforded by the deployment of new imagers at Rankin Inlet and Resolute Bay are being capitalized on in initial studies involving NORSTAR data. For example, PBIs (Poleward Boundary Intensifications) are transient enhancements of the aurora at the boundary between open and closed field lines. They are occasionally periodic ($\tau \approx 5$ minutes) and sometimes extend equatorward after their initial formation. PBIs have been identified and studied almost exclusively in CANOPUS MSP keograms. Hence, little is known of their azimuthal structure, and there is ambiguity about whether PBIs are auroral streamers and/or auroral arcs. Elucidating this two dimensional structure of PBIs is an important goal, as it will provide crucial information about the causal relationship between activity at the distant neutral line and the formation of auroral arcs as well as the generation BBFs. Figure 4 is a keogram of MSP data from Rankin Inlet, showing a clear sequence of PBIs. The NIR image in Figure 5 was obtained with the Rankin Inlet ASI at the time indicated by the vertical white line in Figure 4. At least in this instance, the PBI that occurred just preceding the time of the image was actually the formation of a east-west oriented discrete auroral arc, that subsequently and rapidly propagated equatorward through the CPS.

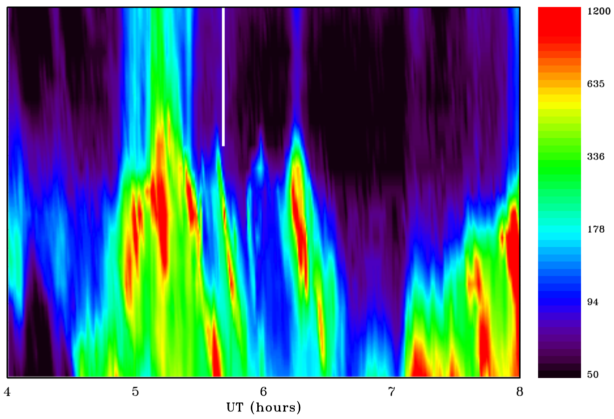

Fig. 4. Keogram of Rankin Inlet MSP 558 nm data (North is up) obtained on 000925 showing a sequence of equatorward extending PBIs. The vertical white line at 0541 UT indicates the time at which the image in Fig. 5 was obtained. Intensities are in Rayleighs.

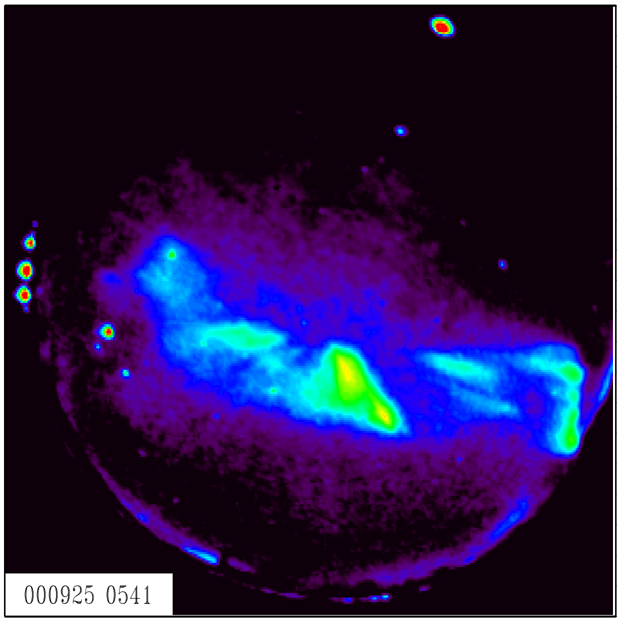

Fig. 5. Rankin Inlet ASI NIR image (North and East are up and right, respectively) showing an equatorward moving East-West arc that is seen as the equatorward extending PBI indicated by the vertical white line in Fig 4.

3.1 NORSTAR IMAGERS

Our current generation of ASIs employ fast all-sky (fish-eye) lenses, yielding a 180° field of view, and intensified 512×512 scientific-grade CCDs to image weak auroral emissions simultaneously from horizon-to-horizon. The optical system was designed and custom built by KEO Consultants (Brookline, MA, USA). High optical throughput is obtained by using fast lenses throughout the optical chain, 3-inch diameter optics, and high-transmittance interference filters. Five-position filter-wheels accommodate filters with passbands centered on (currently) 427.8 nm, 470.9 nm, 486.1 nm (ie, the proton auroral H_β line), 630.0 nm, as well as a background filter (480.6 nm) and high-pass NIR (for Near InfraRed) filter. High sensitivity and corresponding high low-light-level spatial resolution (less than a kilometer at auroral altitudes) are achieved by adopting a special cooled, thinned "blue-enhanced" intensifier photocathode material and a customized fast phosphor at the image intensifier anode. The resulting image is digitized at 16 bits per pixel, giving a fairly large dynamic range, permitting the detection of both faint H_β and 427.8 nm emissions, as well as the more intense NIR and red-line features. Shutter operation, filter-wheel position/temperature, intensifier power and gain, image integration and acquisition, as well as other housekeeping data (such as GPS/UPS parameters), are managed and monitored by a dedicated Linux workstation. Full-resolution images, along with headers containing GPS time stamps, are losslessly compressed and saved onto 4-mm digital tape.

In defining the technical specifications of the first generation of NORSTAR imagers, we hoped for sensitivities that would allow for imaging of low-brightness emissions, such as the 486 nm proton aurora, the 427.8 nm and 470.9 nm N_2^+ bands, and the diffuse oxygen red-line. In Figure 6, we show keograms of oxygen red-line emissions observed simultaneously by the Rankin Inlet MSP and ASI. Though we have not yet determined absolute brightnesses of the ASI data (the calibration exercise discussed below is not complete), we do have absolute brightnesses from the photometer data. Comparison of the two keograms shows that the imager is clearly detecting 100 Rayleigh features, and changes in brightness that are significantly smaller than 100 Rayleighs.

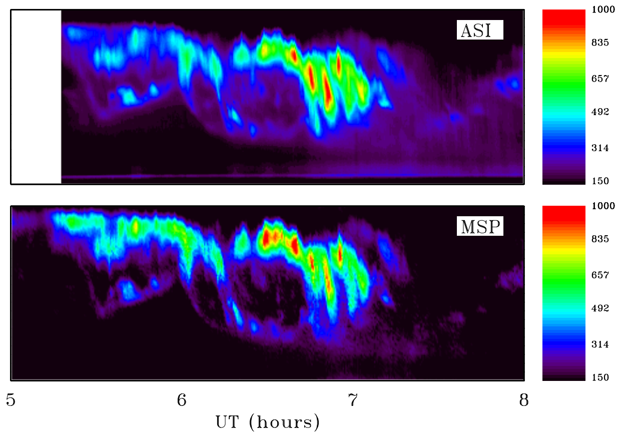

Fig. 6. Keograms (North is up) of Rankin Inlet MSP and ASI 630 nm data obtained on 010102. MSP intensities are in Rayleighs. ASI intensities are autoscaled onto the MSP intensity scale (ie, we have not applied our calibration numbers to the ASI data to create this figure).

3.2 Calibration

Imager calibration allows the conversion of raw Data Numbers (dn) to Rayleighs. The output of the calibration analysis are a flat-field image for each camera and the so-called "R" values (dn/R/sec), the imagers' instrumental responsivities; one value is generated for each filter used on each imager. Two pieces of information are required: the absolute response of the imager to a source of known brightness, and the effective bandwidth of the filter/camera system. The first data are taken by setting up our standard low-brightness source (LBS), in front of (in the zenith of) the imager. Data are taken by exposing 10 images at each of several LBS aperture settings. We use our field operating exposure times. The bandwidth data are taken by pointing the imager at a piece of white, translucent paper, illuminated by a beam of collimated light produced by our monochromator. The paper is turned 45 degrees so it can be seen by the imager. Five images of the target are taken for each of a number of wavelength points, creating a scan of relative intensities through the passband of the filter. Dark frames (same exposure, shutter closed), are taken before and after each data-taking operation. All the resulting data are then analyzed using purpose-written software, and the final "R" values are calculated as

$$R[\mathrm{dn/R/sec}] = \frac{S\,K}{T_{ext}\,B_{lbs}\,A_{lbs}\,BW_{eff}} \quad (1)$$

where S is the imager raw signal response obtained from the dark subtracted LBS data, T_{ext} is the image exposure time in seconds, B_{lbs} is the spectral brightness of the LBS at the filter wavelength, A_{lbs} is the LBS attenuation factor, BW_{eff} is the filter effective bandwidth, and K is the ratio of filter response at emission line to peak filter response ($K = 1.0$ for non-emission-line wavelengths). The latter is determined visually by plotting the measured filter response curve and establishing where the emission line falls. At the time of writing of this paper, we have not completed our calibration of the NORSTAR imagers. In the near future, we will carry out an in depth quantitative comparison of brightnesses obtained from our calibrated imagers and those obtained from the CANOPUS MSPs (ie., see Figure 6).

4 Summary

The CANOPUS ASI operated for fifteen years, with a field of view overlapping (at various times) the CANOPUS magnetometer, riometer, and photometer array, and the BARS VHF radar. The high resolution subset of the CANOPUS ASI data spans the years from 1992 until the imager was decommissioned in the spring of 2001. Three new imagers began operating in 2000, forming the first phase of the NORSTAR program. The CANOPUS ASI data has been instrumental in numerous auroral studies. Data from these new imagers, as well as the original CANOPUS ASI, will provide excellent opportunities for future work.

Acknowledgements. The Gillam ASI and Rankin Inlet MSP are part of the Canadian Space Agency's CANOPUS array. The scientist responsible for the Rankin Inlet MSP is Fokke Creutzberg. Funding for the NORSTAR imagers has been provided by the Province of Alberta Intellectual Infrastucture Partnership Program, and the Natural Sciences and Engineering Research Council (Canada) Equipment Grant and Collaborative Research Grant programs. We acknowledge the crucial support provided by Stanford Research Institute and the Canadian SuperDARN team who have provided us with excellent facilities for the operation of the Resolute Bay and Rankin Inlet imagers, respectively.

References

G. Hall, D. R. Moorcroft, L. L. Cogger, and D. Andre, *J. Geophys. Res.*, 15,281, 1990.

D.J. Knudsen, E.F. Donovan, L.L. Cogger, B. Jackel, and W.D. Shaw, *Geophys. Res. Lett.*, 28, No. 4, 705, 2001.

G. Haerendel, H. U. Frey, O. H. Bauer, E. Rieger, J. Clemmons, M. H. Boehm, D. D. Wallis, and H. Luhr, *Geophys. Res. Lett.*, 21, 1891, 1994

Q. Pao, L. L. Cogger, D. D. Wallis, and A. G. McNamara, *Can. J. Phys.*, 69, 1047, 1991.

P. Prikryl, and L. L. Cogger, *Radio Sci.*, 27, 469, 1991.

G. Rostoker, J. C. Samson, F. Creutzberg, T. J. Hughes, D. R. McDiarmid, A. G. McNamara, A. Vallance Jones, D. D. Wallis, L. L. Cogger, *Space Sci. Rev.*, 71, 743, 1995.

J. C. Samson, L. L. Cogger, and Q. Pao, *J. Geophys. Res.*, 101, 17,373, 1996.

M. T. Syrjäsuo, and E. F. Donovan, *Geophysica*, 38, 3, 2002.

I. Voronkov, E. F. Donovan, B. J. Jackel, and J. C. Samson, *J. Geophys. Res.*, 105, 18,505, 2000.

I. Voronkov, E. Friedrich, and J. C. Samson, *J. Geophys. Res.*, 104, 17,323, 1999.

E. Zesta, L. R. Lyons, and E. Donovan, *Geophys. Res. Lett.*, 27, 3241, 2000.